

RESEARCH

Open Access



# Digital video stabilization based on adaptive camera trajectory smoothing

Marcos R. Souza and Helio Pedrini\*

## Abstract

The development of multimedia equipments has allowed a significant growth in the production of videos through professional and amateur cameras, smartphones, and other mobile devices. Examples of applications involving video processing and analysis include surveillance and security, telemedicine, entertainment, teaching, and robotics. Video stabilization refers to the set of techniques required to detect and correct glitches or instabilities caused during the video acquisition process due to vibrations and undesired motion when handling the camera. In this work, we propose and evaluate a novel approach to video stabilization based on an adaptive Gaussian filter to smooth the camera trajectories. Experiments conducted on several video sequences demonstrate the effectiveness of the method, which generates videos with adequate trade-off between stabilization rate and amount of frame pixels. Our results were compared to YouTube's state-of-the-art method, achieving competitive results.

**Keywords:** Video stabilization, Interest points, Trajectory smoothing, Video processing

## 1 Introduction

The availability of new digital technologies [1–8] and the reduction of equipment costs have facilitated the generation of large volumes of videos in high resolutions. Several devices have allowed the acquisition and editing of videos, such as digital cameras, smartphones, and other mobile devices.

A large number of applications involve the use of digital videos such as telemedicine, advertising, entertainment, robotics, teaching, autonomous vehicles, surveillance, and security. Due to the large amount of video that are captured, stored, and transmitted, it is fundamental to investigate and develop efficient multimedia processing and analysis techniques for indexing, browsing, and retrieving video content [9–11].

Video stabilization [12–21] aims to correct camera motion oscillations that occur in the acquisition process, particularly when the cameras are mobile and handled by amateurs.

Several low-pass filters have been employed in the stabilization process [20, 22]. However, their straightforward application using fixed intensity along all the videos is not suitable, since the camera motion may be unduly

corrected when it should not. Recent approaches have used optimizations [23, 24] to control the local smoothing intensity.

As a main contribution, this work presents and evaluates a novel technique for video stabilization based on an adaptive Gaussian filter to smooth the camera trajectories. Experiments demonstrate the effectiveness of the method, which generates videos with proper stabilization rate while maintaining a reasonable amount of frame pixels.

The proposed method can be seen as an alternative to optimization approaches recently developed in the literature [23, 24] with a lower computational cost. The results are compared to different versions of Gaussian filter, Kalman filter, and the video stabilization method employed in YouTube [24], which is considered a state-of-the-art approach.

This paper is organized as follows. Some relevant concepts and related work are briefly described in Section 2. The proposed method for video stabilization is detailed in Section 3. Experimental results are presented and discussed in Section 4. Finally, some final remarks and directions for future work are included in Section 5.

\*Correspondence: [helio@ic.unicamp.br](mailto:helio@ic.unicamp.br)

Institute of Computing, University of Campinas, Av. Albert Einstein 1251, Campinas 13083-852, Brazil

## 2 Background

Different categories of stabilization approaches [25–32] have been developed to improve the quality of videos, which can be broadly classified as mechanical stabilization, optical stabilization, and digital stabilization.

Mechanical stabilization typically uses sensors to detect camera shifts and compensate for undesired motion. A common way is to use gyroscopes to detect motion and send signals to motors connected to small wheels so that the camera can move in the opposite direction of motion. The camera is usually positioned on a tripod. Despite the efficiency usually obtained with this type of system, there are disadvantages in relation to the resources required, such as device weight and battery consumption.

Optical stabilization [33] is widely used in photographic cameras and consists of a mechanism to compensate for the angular and translational motion of the cameras, stabilizing the image before it is recorded on the sensor. A mechanism for optical stabilization introduces a gyroscope to measure velocity differences at distinct instants in order to distinguish between normal and undesired motion. Other systems employ a set of lenses and sensors to detect angle and speed of motion for video stabilization.

Digital stabilization of videos is implemented without the use of special devices. In general, undesired camera motion is estimated by comparing consecutive frames and applying a transform to the video sequence to compensate for motion. These techniques are typically slower when compared to optical techniques; however, they can achieve adequate results in terms of quality and speed, depending on the algorithms used.

Methods found in the literature for digitally stabilizing videos are usually classified into two-dimensional (2D) or three-dimensional (3D) categories. Sequences of 2D transformations are employed in the first category to represent camera motion and stabilize the videos. Low-pass filters can be used to smooth the transformations, reducing the influence of high frequency of the camera [20, 22]. In the second category, camera trajectories are reconstructed from 3D transformations [34, 35], such as scaling, translation, and rotation.

Approaches that use 2D transformations focus on contributing to specific steps in their stabilization process [36]. By considering the estimation of camera motion, 2D methods can be further subdivided into two categories [32]: (i) intensity-based approaches [37, 38], which directly use the texture of the images as motion vector, and (ii) keypoint-based approaches [39, 40], which locate a set of corresponding points in adjacent frames. Since keypoint-based approaches have a lower computational cost, they are most commonly used [22]. Techniques such as the extraction of regions of interest can be used in this step, in order to avoid cutting certain objects or regions that are supposed to be important to the observer [41].

Many methods have employed different motion filtering mechanisms, such as motion vector integration [39], Kalman filter [42, 43], particle filter [44], and regularization [37]. Such mechanisms aim to remove high-frequency instability from camera motion [36]. Other approaches have focused on improving the quality of the videos, often lost in the stabilization process. The most commonly used techniques include inpainting to fill missing frame parts [22, 41, 45], deconvolution to improve the video focus [22, 41], and weighting of stabilization metrics and video quality aspects [36, 45].

Recent improvements in 2D methods have made them comparable to 3D methods in terms of quality. For instance, the use of an L1-norm optimization can generate a camera path that follows cinematographic rules in order to consider separately constant, linear, and parabolic motion [24]. A mesh-based model, in which multiple trajectories are calculated at different locations of the video, proved to be efficient in dealing with parallax without the use of 3D methods [23]. A semi-automatic 2D method, which requires assistance from the user, is proposed to adjust problematic frames [46].

On the other hand, 3D methods typically construct a three-dimensional model of the scene through structure-from-motion (SFM) techniques for smoothing motion [47], providing superior quality stabilization but at a higher computational cost [27, 47]. Since they usually have serious problems in handling large objects in the foreground [36], 2D methods are in general preferred in practice [36].

Although 3D methods can generate good results in static scenes using image-based rendering techniques [34, 48], they usually do not handle dynamic scenes correctly, causing motion blur [49]. Thus, the concept of content preservation was introduced, restricting each output frame to be generated from a single input frame [49]. Other approaches address this problem through a geometric approximation by abdicating to be robust with respect to the parallax [35]. Other difficulties found in 3D methods appear in amateur videos, such as lack of parallax, zoom, and use of complementary metal oxide semiconductor (CMOS) sensors, among others [47].

Although not common, 3D methods can fill missing parts of a frame by using information from several other frames [48]. More recently, 2D and 3D methods have been extended to deal with stereoscopic videos [29, 50]. Hybrid approaches have emerged to obtain the efficiency and robustness of 2D methods in addition to the high quality of 3D methods. Some of them are based on concepts such as trajectories subspace [47] and epipolar transfer [51]. A hybrid method for dealing with discrete depth variations present in short-distance videos was described by Liu et al. [31].

### 3 Adaptive video stabilization method

This section presents the proposed video stabilization method based on an adaptive Gaussian smoothing of the camera trajectories. Figure 1 illustrates the main stages of the methodology, which are described in the following subsections.

#### 3.1 Keypoint detection and matching

The process starts with the detection and description of keypoints in the video frames. In this step, we used the speeded up robust features (SURF) method [52]. After extracting the keypoints between two adjacent frames, their correspondence is performed using the brute-force method with cross-checking, where the Euclidean distance between the feature vectors for each pair of points  $x_i \in f_t$  and  $x'_j \in f_{t+1}$  is calculated for two adjacent frames  $f_t$  and  $f_{t+1}$ . Thus,  $x_i$  corresponds to  $x'_j$  if and only if  $x_i$  is the closest point to  $x'_j$  and  $x'_j$  the closest to  $x_i$ .

Figures 2 and 3 show the detection of keypoints in a frame and the correspondence between the points of two adjacent superimposed frames, respectively.

#### 3.2 Motion estimation

After determining the matches between the keypoints, it is necessary to estimate the motion performed by the camera. For this, we estimate the similarity matrix, that is, the matrix that transforms the set of points in a frame  $f_t$  to the set of points in a frame  $f_{t+1}$ . Since we consider the matrix of similarity, the parameters of the matrix transformation take into account camera shifts (translation), distortion (scaling), and undesirable motion (rotation) for the construction of a stabilization model.

In the process of digital video stabilization, oscillations of the camera that occurred at the time of recording must be compensated. The similarity matrix should take into account only the correspondences that are, in fact, between two equivalent points. In addition, it should not consider the movement of objects present in the scene.

The random sample consensus (RANSAC) method is applied to estimate a similarity matrix that considers only inliers in order to disregard the incorrect correspondences

and those that describe the movement of objects. In the application of this method, the value of the residual threshold parameter, which determines the maximum error for a match to be considered as inlier, is calculated for each pair of frames. Algorithm 1 presents the calculation to determine the final similarity matrix.

---

#### Algorithm 1 Similarity matrix computation

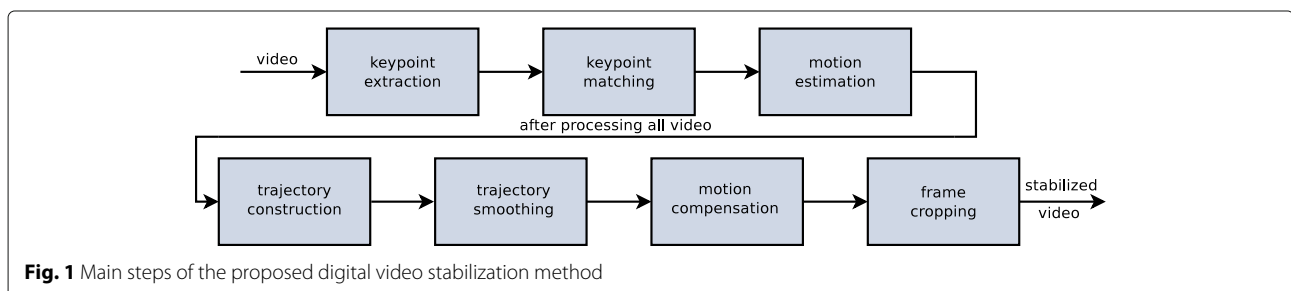
---

- 1: **procedure** FINALMATRIX
  - 2:   Generate the similarity matrix  $M$  by considering all matches.
  - 3:   Let  $MSE(M)$  be the mean square error of matrix  $M$ .
  - 4:   Apply the RANSAC considering the  $MSE(M)$  as residual threshold value.
  - 5:   Generate the similarity matrix  $M'$  considering only the inliers obtained previously.
  - 6:   Let  $MSE(M')$  be the mean square error of matrix  $M'$ .
  - 7:   Apply the RANSAC considering the  $MSE(M')$  as residual threshold value.
  - 8:   Generate the similarity matrix  $M_{final}$  considering only the inliers obtained for the second execution of RANSAC.
- 

In cases of pairs of frames with spatially variant motion, the correct matches also tend to have certain variation. Thus, the residual threshold is calculated so that its value is low enough to eliminate undesired matches and high enough such that the correct matches are maintained.

#### 3.3 Trajectory construction

After estimating the final similarity matrices for each pair of adjacent frames of the video, a trajectory is calculated for each of the factors of the similarity matrix. In this work, we consider a vertical translation factor, a horizontal translation factor, a rotation factor, and a scaling factor. Each factor  $f$  of the matrix is decomposed, and the trajectory of each of them is calculated in order to accumulate its previous values, expressed as



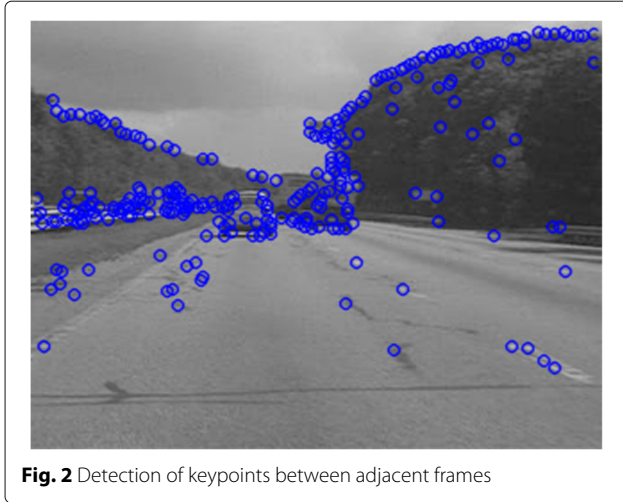


**Fig. 2** Detection of keypoints between adjacent frames

$$t_i^f = t_{i-1}^f + \Delta_i^f \tag{1}$$

where  $t_i$  is the value of a given trajectory in the  $i$ -th position and  $\Delta_i^f$  is the value of the factor  $f$  for the  $i$ -th similarity matrix previously estimated. The trajectories are then smoothed. The equations presented in the remainder of the text are always applied to the trajectories of each factor separately. Thus, the factor index  $f$  will be omitted in order to not overload the notation.

### 3.4 Trajectory smoothing

Assuming that only the camera motion is present in the similarity matrices, the calculated trajectory refers to the path made by the camera during the video recording. To obtain a stabilized video, it is necessary to remove the oscillations from this path, keeping only the desired motion.

Since the Gaussian filter is a linear low-pass filter, it attenuates the high frequencies present in a signal. The

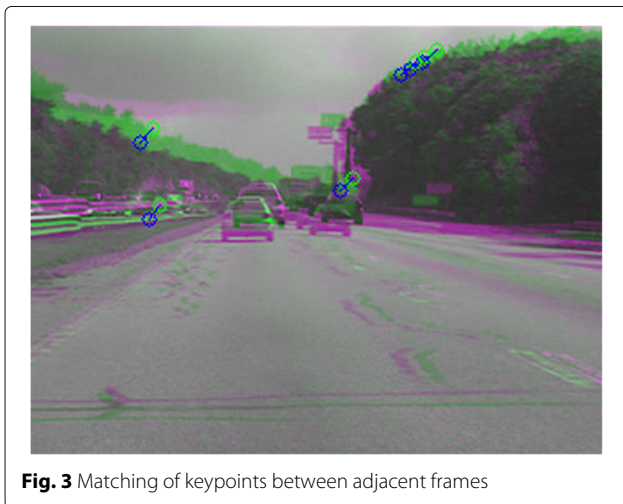


**Fig. 3** Matching of keypoints between adjacent frames

Gaussian filter modifies the input through a convolution by considering a Gaussian function in a window of size  $M$ . Thus, this function is used as impulse response in the Gaussian filter and can be defined as

$$G(x) = ae^{-\frac{(x-\mu)^2}{2\sigma^2}} \tag{2}$$

where  $a$  is a constant considered as 1 so that  $G(x)$  has values between 0 and 1. The constant  $\mu$  is the expected value, considered as 0, whereas  $\sigma^2$  represents the variance.

The parameter  $M$  indicates the number of points of the output window, whose value is expressed as

$$M = \frac{n}{3} - 1 \tag{3}$$

where  $n$  is the total number of frames in the video.

Since different instants of the video will have a distinct amount of oscillations, this work applies a Gaussian filter adaptively in order to remove only the undesired camera motion.

The smoothing of an intense motion may result in videos with a low amount of pixels. Moreover, this type of motion is typically a desired camera motion, which should not be smoothed. Therefore, the parameter  $\sigma$  is computed in such a way that it has smaller values in these regions. Thus, the trajectory will be smoothed by considering a distinct value for  $\sigma_i$  at each point  $i$ . To determine the value of  $\sigma_i$ , a sliding window of size twice as large as the frame rate measure is applied, so that the window information lasts for two video seconds. The ratio  $r_i$  is expressed as

$$r_i = \left(1 - \frac{\mu_i}{max\_value}\right)^2 \tag{4}$$

where the *max\_value* corresponds to either width in the horizontal translation trajectory or height in the vertical translation trajectory. In this work, we consider  $\theta = \frac{\pi}{6}$  as the angle (in radians) in the rotation trajectory. Thus, the motion will be considered large based mainly on the video resolution. Value  $\mu_i$  is calculated in such a way to give higher weights to points closer to  $i$ , where  $\mu_i$  is expressed as

$$\mu_i = \frac{\sum_{j \in W_i, j \neq i} G(|j-i|, \sigma_\mu) \Delta_j}{\sum_{j \in W_i} G(|j-i|, \sigma_\mu)} \tag{5}$$

where  $j$  is the index of each point in the window of  $i$ , whereas  $G()$  is a Gaussian function with  $\sigma$  calculated as

$$\sigma_\mu = FPS(1 - CV) \tag{6}$$

where FPS is the video frames per second, and CV is the coefficient of variation of the absolute values of the trajectory that are inside the window. As the value of CV is between 0 and 1, its final value is limited

to 0.9 in order for  $\sigma_\mu$  not to have null values. Therefore,  $\sigma_\mu$  makes the actual size of the window adaptive, such that the higher the variation of motion inside the window, the higher the weight given to the central points.

The coefficient of variation can be expressed as

$$CV = \frac{std(\forall t_i | i \in W_i)}{avg(\forall t_i | i \in W_i)} \tag{7}$$

where  $W_i$  is in the same window as in Eq. 5 and  $t_i$  the trajectory value. Therefore, the coefficient of variation corresponds to the standard deviation *std* to the average *avg*.

Assuming that  $r_i$  ranges between 0 and 1, a linear transformation is applied to obtain a proper interval to the Gaussian filter. This transformation is given as

$$\sigma_i = \frac{\sigma_{max} - \sigma_{min}}{r_{max} - r_{min}} (r_i - r_{min}) + \sigma_{min} \tag{8}$$

where  $\sigma_{min}$  and  $\sigma_{max}$  are the minimum and maximum values of the new interval (after linear transformation), respectively. In this work, these values are defined as 0.5 and 40, respectively. Values  $r_{min}$  and  $r_{max}$  are the minimum and maximum values of the old interval (before linear transformation). In this work, value  $r_{max}$  is always set to 1. To control whether a motion is desired or not, a value in the interval between 0 and 1 is set to  $r_{min}$ . The same  $r_{min}$  is used as a lower limit to  $r_i$ , before applying the linear transformation.

An exponential transformation is then applied to  $\sigma_i$  values to amplify their magnitude. After calculating  $\sigma_i$  for each point of the trajectory, its values are lightly smoothed by a Gaussian filter with  $\sigma = 5$ , chosen empirically. This is done to avoid abrupt changes in the value of  $\sigma_i$  along the trajectory. Finally, the Gaussian filter is applied  $n$  times (once for each point in the trajectory), generating a

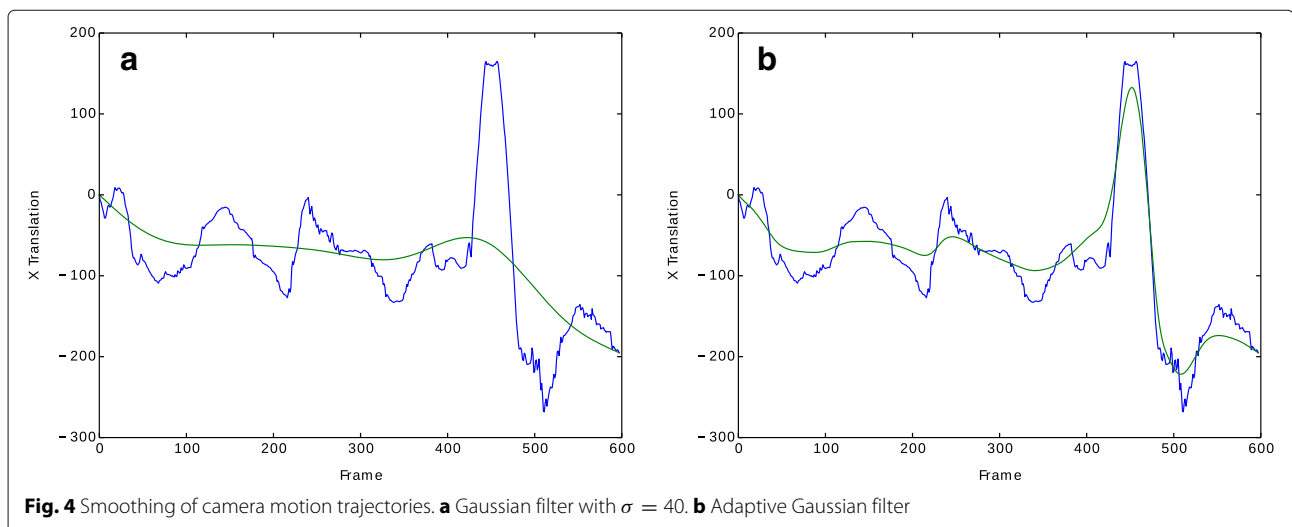
smoothed trajectory (indexed by  $k$ ) for each  $\sigma_i$  previously calculated. The final smoothed trajectory corresponds to the concatenation of points for each of the generated trajectories, and the  $k$ -th trajectory contributes with its  $k$ -th point. Thus, an adaptive smoothed path is obtained. This process is applied only to the translation and rotation paths.

Figure 4 shows the trajectory generated by considering the horizontal translational factor (blue) and the obtained smoothing (green) using the Gaussian filter with  $\sigma = 40$  and the adaptive version proposed in this work. It is possible to observe that the smoothing is applied at different degrees along the trajectory.

### 3.5 Motion compensation and frame cropping

After applying the Gaussian filter, it is necessary to recalculate the value of each factor for each similarity matrix. In order to do that, the similarity matrix value of a given factor is calculated by the difference between each point of its smoothed trajectory and its predecessor. With the similarity matrices of each pair of frames updated, the similarity matrix is applied to the first frame of the pair to take it to the coordinates of the second.

Applying the geometric transformation in the frame causes information to be lost in certain pixels of the frame boundary. Figure 5 presents a transformed frame, where it is possible to observe the loss of information at the borders. They are then cropped so that no frames in the stabilized video hold pixels without information. To determine the frame boundaries, each similarity matrix is applied to the original coordinates of the four vertices, thus generating the transformed coordinates for the respective frame. Finally, the innermost coordinates of all frames are considered final. Figure 6, extracted from [22], illustrates the cropping process applied to the transformed frame.



**Fig. 4** Smoothing of camera motion trajectories. **a** Gaussian filter with  $\sigma = 40$ . **b** Adaptive Gaussian filter



**Fig. 5** Frame after application of geometric transformation

### 3.6 Evaluation metrics

The peak signal-to-noise ratio (PSNR) is used to evaluate the overall difference between two frames of the video, expressed as

$$\text{PSNR}(f_t, f_{t+1}) = 10 \log_{10} \frac{WHL_{\max}^2}{\sum_{x=1}^W \sum_{y=1}^H [f_t(x, y) - f_{t+1}(x, y)]^2} \quad (9)$$

where  $f_t$  and  $f_{t+1}$  are two consecutive frames of the video,  $W$  and  $H$  are the width and height of each frame, respectively, and  $L_{\max}$  is the maximum value intensity of the image. The PSNR metric is expressed in decibel (dB), a unit originally defined to measure sound intensity on a logarithmic scale. Typical PSNR values range from 20 to 40. The PSNR value should increase from the initial

video sequence to the stabilized sequence, since frames after transformation will tend to be more similar.

The interframe transformation fidelity (ITF) can be used to evaluate the final stabilization of the method, expressed as

$$\text{ITF} = \frac{1}{N-1} \sum_{k=1}^{N-1} \text{PSNR}(k) \quad (10)$$

where  $N$  is the number of frames in the videos. Typically, the stabilized sequence has a higher ITF value than the original sequence.

Due to the loss of information in the application of the similarity matrix in the frames, it is important to evaluate and compare such rate among different stabilization methods. For this, we report the percentage of pixels held by the stabilized video in comparison to the original video, expressed as

$$\text{Rate of preserved pixels} = 100 \frac{W_s H_s}{WH} \quad (11)$$

where  $W$  and  $H$  correspond to the width and height of the frames in the original video and  $W_s$  and  $H_s$  correspond to the width and height of the frames in the video generated by the stabilization process, respectively.

## 4 Results and discussion

This section describes the results of experiments conducted on a set of input videos. Fourteen videos with oscillations were submitted to the stabilization process and evaluated, where eleven of them are available from the



**Fig. 6** Frame after boundary cropping

**Table 1** Video sequences used in our experiments

No.	Video	Source	Resolution (pixels)	FPS
1	gleicher1	GaTech VideoStab	640 × 360	30
2	gleicher2	GaTech VideoStab	640 × 360	30
3	gleicher3	GaTech VideoStab	640 × 360	30
4	gleicher4	GaTech VideoStab	640 × 360	30
5	greyson_chance	GaTech VideoStab	640 × 360	30
6	hippo	nghiaho.com/uploads/hippo.mp4	480 × 360	30
7	lf_juggle	GaTech VideoStab	480 × 360	25
8	new_gleicher	GaTech VideoStab	480 × 270	30
9	sam_1	GaTech VideoStab	640 × 360	30
10	sam and cocoa	youtu.be/627MqC6E5Yo	540 × 360	30
11	sany0025	GaTech VideoStab	640 × 360	30
12	shake_pgh_1	GaTech VideoStab	640 × 360	30
13	shaky_car	MatLab	320 × 240	30
14	yuna_long	GaTech VideoStab	640 × 360	30

GaTech VideoStab [24] database and the three others collected separately. Table 1 presents the videos used in the experiments and their sources.

In the experiments performed, we compared the values of the ITF metric as well as the amount of pixels held for different versions of the trajectory smoothing. In the first version, we used the Gaussian filter considering  $\sigma = 40$ . In another version, the Gaussian filter is used in a slightly more adaptive way, choosing different values of  $\sigma$

for each trajectory according to the size of the trajectory range with respect to the size of the video frame. Higher values of  $\sigma$  are assigned to paths with smaller intervals; we then denominate this version as semi-adaptive. The locally adaptive version of the Gaussian filter proposed in this work is presented. A version using the Kalman filter is also shown. In addition, the videos were submitted to the YouTube stabilization method [24] in order to compare its results against ours. The metric is calculated for

**Table 2** Comparison between Gaussian filter and Kalman filter

No. of videos	Original	Gaussian filter $\sigma = 40$		Kalman filter	
	ITF	ITF	Hold pixels (%)	ITF	Hold pixels (%)
1	18.793	27.738	69.276	25.888	71.000
2	20.390	29.331	71.750	27.201	74.771
3	16.186	22.559	72.972	22.122	73.003
4	19.965	33.380	48.958	26.298	54.903
5	23.277	28.660	2.540	25.991	4.958
6	19.681	29.804	67.891	25.576	73.507
7	24.109	28.510	60.495	28.063	57.167
8	17.881	25.448	70.648	24.081	72.287
9	19.248	23.251	25.797	21.426	33.818
10	12.972	18.453	17.519	16.680	27.204
11	21.487	26.826	43.599	25.704	52.875
12	15.081	0	0	20.219	2.686
13	23.841	30.621	70.312	28.200	71.875
14	18.065	20.265	7.448	20.902	7.642
Average	19.355	24.631	44.953	24.167	48.406

**Table 3** Comparison between semi-adaptive Gaussian filter and adaptive Gaussian filter

No. of videos	Original	Semi-adaptive Gaussian filter		Locally adaptive Gaussian filter	
	ITF	ITF	Hold pixels (%)	ITF	Hold pixels (%)
1	18.793	27.620	70.745	27.455	74.500
2	20.390	29.331	71.750	28.914	75.781
3	16.186	22.559	72.972	22.090	76.056
4	19.965	33.380	48.958	27.931	62.465
5	23.277	27.814	8.312	27.360	53.385
6	19.681	29.804	67.891	29.077	70.838
7	24.109	28.510	60.495	28.876	73.667
8	17.881	25.448	70.648	25.182	73.284
9	19.248	21.845	35.750	21.435	57.139
10	12.972	17.465	27.907	16.381	70.296
11	21.487	26.826	43.559	25.659	57.260
12	15.081	19.827	16.611	17.895	59.847
13	23.841	30.621	70.312	29.987	71.719
14	18.065	19.759	39.045	19.773	54.146
Average	19.355	25.772	50.353	24.858	66.455

the video sequence before and after the stabilization process. Table 2 shows the results obtained with the Kalman filter and the Gaussian filter with  $\sigma = 40$ .

From Table 2, we can observe a certain superiority in the use of the Gaussian filter, which achieves a higher ITF value for all videos with basically the same amount of pixels kept for most videos. Videos #5, #9, #10, #12, and #14 keep a lower amount of pixels compared to the other videos. This is due to the presence of desired

camera motion, which is erroneously considered as oscillations by the Gaussian filter, if the value of  $\sigma$  used is high enough. However, smaller values may not remove the oscillations from the videos efficiently, since each video has oscillations of different proportions.

In order to improve the quality of the stabilization for these cases, Table 3 presents the results obtained with the version of the semi-adaptive Gaussian filter, where trajectories with greater difference between the

**Table 4** Comparison between adaptive Gaussian filter and YouTube method [24]

No. of videos	Original	Locally adaptive Gaussian filter	YouTube [24]	Hold pixels
1	18.793	27.455	27.890	Superior
2	20.390	28.914	28.604	Superior
3	16.186	22.090	23.030	Comparable
4	19.965	27.931	33.711	Superior
5	23.277	27.360	27.599	Inferior
6	19.681	29.077	29.390	Superior
7	24.109	28.876	29.252	Comparable
8	17.881	25.182	25.908	Superior
9	19.248	21.435	20.922	Inferior
10	12.972	16.381	20.495	Superior
11	21.487	25.659	26.672	Comparable
12	15.081	17.895	19.283	Comparable
13	23.841	29.987	28.845	Comparable
14	18.065	19.773	20.128	Inferior
Average	19.355	24.858	25.837	–





**Fig. 7** Video #1. Amount of pixels hold through our method is superior than the state-of-the-art approach. **a** Adaptive Gaussian filter; **b** YouTube [24]

minimum and maximum values will have a lower value for  $\sigma$ . We used  $\sigma = 40$  for trajectories with intervals smaller than 80% of the respective frame size, whereas  $\sigma = 20$  otherwise. For the locally adaptive version proposed in this work, we experimentally set  $r_{\min}$  as 0.4, whose results are reported in Table 3.

The semi-adaptive version maintains more pixels in the videos in which the original Gaussian filter had problems, since  $\sigma = 20$  was applied to them. However, the amount of pixels held in the frames is lower than in the other videos. This is because, in many cases,  $\sigma = 20$  is still a very high value. On the other hand, smaller values of  $\sigma$  can ignore the oscillations that are present in other instance of the video, thus generating videos not stabilized enough and consequently with a lower ITF value. Therefore, as can be seen in Table 3, the locally adaptive version, whose smoothing intensity is changed along the trajectory, obtained ITF values comparable to the original and semi-adaptive version, maintaining considerably more pixels.

Table 4 presents a comparison of the results between our method and YouTube approach [24]. The percentage of pixels held was not reported since the YouTube method resizes the stabilized videos to their original size. Thus, a qualitative analysis is done through the first frame of each video, whose results are classified into three categories: superior (when our method maintains more pixels), inferior (when the YouTube method holds more pixels), and

comparable (when both methods hold basically the same amount of pixels). Figures 7, 8, and 9 illustrate the analysis performed.

In Fig. 7, it is possible to observe that more information is maintained on the top, left, and right sides of the video obtained with our method. The difference is not considerably large, and the advantage or disadvantage obtained follows these proportions in most videos.

In Fig. 8, there is less information maintained on the top and bottom sides in the use of the adaptive Gaussian filter. On the other hand, there is a larger amount of information held on the left and right sides.

Figure 9 illustrates a situation where our method maintains less pixels. Lower amount of information is held on the every sides with our method.

From Table 4, we can observe a certain parity for both methods in terms of ITF metric, with a slight advantage of the YouTube method [24], while the maintained pixels are in general comparable and, when lower, do not differ much. This demonstrates that the proposed method is competitive with one of the methods considered as current state-of-the-art, despite the simplicity of our method. Notwithstanding, the method still needs to be further extended to deal with some adverse situations, such as the treatment of non-rigid oscillations in the video #10, the rolling shutter in the video #12, and the parallax effect, among others.



**Fig. 8** Video #3. Amount of pixels hold through our method is comparable to the state-of-the-art approach. **a** Adaptive Gaussian filter; **b** YouTube [24]



**Fig. 9** Video #12. Amount of pixels hold through our method is inferior than the state-of-the-art approach. **a** Adaptive Gaussian filter; **b** YouTube [24]

## 5 Conclusions

In this work, we presented a technique for video stabilization based on an adaptive Gaussian filter to smooth the camera trajectory in order to remove undesired oscillations. The proposed filter assigns distinct values to  $\sigma$  along the camera trajectory by considering that the intensity of the oscillations changes throughout the video and that a very high value of  $\sigma$  can result in a video with a low amount of pixels, while smaller values generate less stabilized videos.

The results obtained in the experiments were compared with different versions for the smoothing of the trajectory: Kalman filter, Gaussian filter with  $\sigma = 40$ , and a semi-adaptive Gaussian filter. The approaches achieved comparable values for the ITF metric while maintaining a significantly higher amount of pixels.

A comparison was performed with the stabilization method used in YouTube, where the results were competitive. As directions for future work, we intend to extend our method to deal with some adverse situations, such as non-rigid oscillations and effect of parallax.

### Abbreviations

2D: Two-dimensional; 3D: Three-dimensional; CMOS: Complementary metal oxide semiconductor; CV: Coefficient of variation; dB: Decibel; ITF: Interframe transformation fidelity; MSE: Mean square error; PSNR: Peak signal-to-noise ratio; RANSAC: Random sample consensus; SFM: Structure-from-motion

### Acknowledgements

The authors would like to thank the editors and anonymous reviewers for their valuable comments.

### Funding

The authors are thankful to FAPESP (grants #2014/12236-1 and #2017/12646-3) and CNPq (grant #305169/2015-7) for their financial support.

### Availability of data and materials

Data are publicly available.

### Authors' contributions

HP and MRS contributed equally to this work. Both authors carried out the in-depth analysis of the experimental results and checked the correctness of the evaluation. Both authors took part in the writing and proof reading of the final version of the paper. Both authors read and approved the final manuscript.

### Competing interests

The authors declare that they have no competing interests.

### Publisher's Note

Springer Nature remains neutral with regard to jurisdictional claims in published maps and institutional affiliations.

Received: 28 November 2017 Accepted: 15 May 2018

Published online: 30 May 2018

### References

1. C Yan, Y Zhang, J Xu, F Dai, J Zhang, Q Dai, et al., Efficient parallel framework for HEVC motion estimation on many-core processors. *IEEE Trans. Circ. Syst. Video Technol.* **24**(12), 2077–2089 (2014)
2. MF Alcantara, TP Moreira, H Pedrini, Real-time action recognition using a multilayer descriptor with variable size. *J. Electron. Imaging*, **25**(1), 013020.1?013020.9 (2016)
3. C Yan, Y Zhang, J Xu, F Dai, L Li, Q Dai, et al., A highly parallel framework for HEVC coding unit partitioning tree decision on many-core processors. *IEEE Sig. Process. Lett.* **21**(5), 573–576 (2014)
4. MF Alcantara, H Pedrini, Y Cao, Human action classification based on silhouette indexed interest points for multiple domains. *Int. J. Image Graph.* **17**(3), 1750018\_1–1750018\_27 (1750)
5. C Yan, H Xie, D Yang, J Yin, Y Zhang, Q Dai, Supervised hash coding with deep neural network for environment perception of intelligent vehicles. *IEEE Trans. Intell. Transp. Syst.* **19**(1), 284–295 (2018)
6. MF Alcantara, TP Moreira, H Pedrini, F Flérez-Revuelta, Action identification using a descriptor with autonomous fragments in a multilevel prediction scheme. *Signal Image Video Process.* **11**(2), 325–332 (2017)
7. C Yan, H Xie, S Liu, J Yin, Y Zhang, Q Dai, Effective Uyghur language text detection in complex background images for traffic prompt identification. *IEEE Trans. Intell. Transp. Syst.* **19**(1), 220–229 (2018)
8. BS Torres, H Pedrini, Detection of complex video events through visual rhythm. *Vis. Comput.* **34**(2), 145–165 (2018)
9. MVM Cirne, H Pedrini, in *Progress in Pattern Recognition, Image Analysis, Computer Vision, and Applications. A video summarization method based on spectral clustering* (Springer, 2013), pp. 479–486
10. MVM Cirne, H Pedrini, in *Progress in Pattern Recognition, Image Analysis, Computer Vision, and Applications. Summarization of videos by image quality assessment* (Springer, 2014), pp. 901–908
11. TS Huang, *Image Sequence Analysis. vol. 5.* (Springer Science & Business Media, Heidelberg, 2013)
12. AA Amanatiadis, I Andreadis, Digital image stabilization by independent component analysis. *IEEE Trans. Instrum. Meas.* **59**(7), 1755–1763 (2010)
13. JY Chang, WF Hu, MH Cheng, BS Chang, Digital image translational and rotational motion stabilization using optical flow technique. *IEEE Trans. Consum. Electron.* **48**(1), 108–115 (2002)
14. S Ertürk, Real-time digital image stabilization using Kalman filters. *Real-time Imaging.* **8**(4), 317–328 (2002)
15. R Jia, H Zhang, L Wang, J Li, in *International Conference on Artificial Intelligence and Computational Intelligence. Digital image stabilization based on phase correlation. vol. 3* (IEEE, 2009), pp. 485–489
16. SJ Ko, SH Lee, KH Lee, Digital image stabilizing algorithms based on bit-plane matching. *IEEE Trans. Consum. Electron.* **44**(3), 617–622 (1998)
17. S Kumar, H Azartash, M Biswas, T Nguyen, Real-time affine global motion estimation using phase correlation and its application for digital image stabilization. *IEEE Trans. Image Process.* **20**(12), 3406–3418 (2011)
18. CT Lin, CT Hong, CT Yang, Real-time digital image stabilization system using modified proportional integrated controller. *IEEE Trans. Circ. Syst. Video Technol.* **19**(3), 427–431 (2009)
19. L Marcenaro, G Vernazza, CS Regazzoni, in *International Conference on Image Processing. Image stabilization algorithms for video-surveillance applications. vol. 1* (IEEE, 2001), pp. 349–352

20. C Morimoto, R Chellappa, in *13th International Conference on Pattern Recognition*. Fast electronic digital image stabilization. vol. 3 (IEEE, 1996), pp. 284–288
21. YG Ryu, MJ Chung, Robust online digital image stabilization based on point-feature trajectory without accumulative global motion estimation. *IEEE Signal Proc. Lett.* **19**(4), 223–226 (2012)
22. Y Matsushita, E Ofek, W Ge, X Tang, HY Shum, Full-frame video stabilization with motion inpainting. *IEEE Trans. Pattern Anal. Mach. Intell.* **28**(7), 1150–1163 (2006)
23. S Liu, L Yuan, P Tan, J Sun, Bundled camera paths for video stabilization. *ACM Trans. Graph.* **32**(4), 78 (2013)
24. M Grundmann, V Kwatra, I Essa, in *IEEE Conference on Computer Vision and Pattern Recognition*. Auto-directed video stabilization with robust L1 optimal camera paths (IEEE, 2011), pp. 225–232
25. C Jia, BL Evans, Online motion smoothing for video stabilization via constrained multiple-model estimation. *EURASIP J. Image Video Proc.* **2017**(1), 25 (2017)
26. S Liu, M Li, S Zhu, B Zeng, CodingFlow: enable video coding for video stabilization. *IEEE Trans. Image Proc.* **26**(7), 3291–3302 (2017)
27. Z Zhao, X Ma, in *IEEE International Conference on Image Processing*. Video stabilization based on local trajectories and robust mesh transformation (IEEE, 2016), pp. 4092–4096
28. N Bhowmik, V Gouet-Brunet, L Wei, G Bloch, in *International Conference on Multimedia Modeling*. Adaptive and optimal combination of local features for image retrieval (Springer, Cham, 2017), pp. 76–88
29. H Guo, S Liu, S Zhu, B Zeng, in *IEEE International Conference on Image Processing*. Joint bundled camera paths for stereoscopic video stabilization (IEEE, 2016), pp. 1071–1075
30. Q Zheng, M Yang, A video stabilization method based on inter-frame image matching score. *Glob. J. Comput. Sci. Technol.* **17**(1), 41–46 (2017)
31. S Liu, B Xu, C Deng, S Zhu, B Zeng, M Gabbouj, A hybrid approach for near-range video stabilization. *IEEE Trans. Circ. Syst. Video Technol.* **27**(9), 1922–1933 (2016)
32. BH Chen, A Kopylov, SC Huang, O Seregin, R Karpov, SY Kuo, et al., Improved global motion estimation via motion vector clustering for video stabilization. *Eng. Appl. Artif. Intell.* **54**, 39–48 (2016)
33. B Cardani, Optical Image Stabilization for Digital Cameras. *IEEE Control. Syst.* **26**(2), 21–22 (2006)
34. C Buehler, M Bosse, L McMillan, in *IEEE Computer Society Conference on Computer Vision and Pattern Recognition*. Non-metric image-based rendering for video stabilization. vol. 2 (IEEE, 2001), pp. 11–609
35. G Zhang, W Hua, X Qin, Y Shao, H Bao, Video Stabilization based on a 3D Perspective Camera Model. *Vis. Comput.* **25**(11), 997–1008 (2009)
36. KY Lee, YY Chuang, BY Chen, M Ouhyoung, in *IEEE 12th International Conference on Computer Vision*. Video stabilization using robust feature trajectories (IEEE, 2009), pp. 1397–1404
37. HC Chang, SH Lai, KR Lu, in *IEEE International Conference on Multimedia and Expo*. A robust and efficient video stabilization algorithm. vol. 1 (IEEE, 2004), pp. 29–32
38. G Puglisi, S Battiato, A robust image alignment algorithm for video stabilization purposes. *IEEE Trans. Circ. Syst. Video Technol.* **21**(10), 1390–1400 (2011)
39. S Battiato, G Gallo, G Puglisi, S Scellato, in *14th International Conference on Image Analysis and Processing*. SIFT features tracking for video stabilization (IEEE, 2007), pp. 825–830
40. Y Shen, P Guturu, T Damarla, BP Buckles, KR Namuduri, Video stabilization using principal component analysis and scale invariant feature transform in particle filter framework. *IEEE Trans. Consum. Electron.* **55**(3), 1714–1721 (2009)
41. BY Chen, KY Lee, WT Huang, JS Lin, Wiley Online Library. Capturing intention-based full-frame video stabilization. *Comput. Graphics Forum.* **27**(7), 1805–1814 (2008)
42. S Ertürk, Image sequence stabilisation based on Kalman filtering of frame positions. *Electron. Lett.* **37**(20), 1 (2001)
43. A Litvin, J Konrad, WC Karl, in *Electronic Imaging. International Society for Optics and Photonics*. Probabilistic video stabilization using Kalman filtering and mosaicing (SPIE-IS&T, 2003), pp. 663–674
44. J Yang, D Schonfeld, C Chen, M Mohamed, in *International Conference on Image Processing*. Online video stabilization based on particle filters (IEEE, 2006), pp. 1545–1548
45. ML Gleicher, F Liu, Re-cinematography: improving the camerawork of casual video. *ACM Trans. Multimed. Comput. Commun. Appl.* **5**(1), 2 (2008)
46. J Bai, A Agarwala, M Agrawala, R Ramamoorthi, Wiley Online Library. User-assisted video stabilization. *Comput. Graph. Forum.* **33**(4), 61–70 (2014)
47. F Liu, M Gleicher, J Wang, H Jin, A Agarwala, Subspace video stabilization. *ACM Trans. Graph.* **30**(1), 4 (2011)
48. P Bhat, CL Zitnick, N Snavely, A Agarwala, M Agrawala, M Cohen, et al, in *18th Eurographics Conference on Rendering Techniques. Eurographics Association*. Using photographs to enhance videos of a static scene, (2007), pp. 327–338
49. F Liu, M Gleicher, H Jin, A Agarwala, Content-preserving warps for 3D video stabilization. *ACM Trans. Graph.* **28**(3), 44 (2009)
50. F Liu, Y Niu, H Jin, in *IEEE International Conference on Computer Vision*. Joint subspace stabilization for stereoscopic video, (2013), pp. 73–80
51. A Goldstein, R Fattal, Video stabilization using epipolar geometry. *ACM Trans. Graph.* **31**(5), 1–10 (2012)
52. H Bay, A Ess, T Tuytelaars, L Van Gool, Speeded-up robust features (SURF). *Comput. Vis. Image Underst.* **110**(3), 346–359 (2008)

**Submit your manuscript to a SpringerOpen<sup>®</sup> journal and benefit from:**

- Convenient online submission
- Rigorous peer review
- Open access: articles freely available online
- High visibility within the field
- Retaining the copyright to your article

---

Submit your next manuscript at ► [springeropen.com](http://springeropen.com)